Planets in a terrestrial orbit

In this chapter, we present a study of the thermal emission of four Earth-like planets. We are interested on the effect of its physical characteristics over the climate, the global infrared emission and the shape of the thermal light curve observed at different geometries. The method applied is analogue to the study of the emission of the Earth described in Chapter 4. With the aim of obtaining a variety of climates, we have used LMD Global Climate Model data of four planets with the orbital characteristics and atmospheric composition of the Earth, whereas the rotation rate, the surface or the stellar radiation have been modified in each case. Section 5.1 is an introduction to the climate characteristics of Earth-like planets and presents the parameters used to typify each planet. The results are given in Section 5.2. Then, in Section 5.3, we build and analyze the thermal light curves of each planet. The retrieval of the planetary period is discussed in Section 5.4, and the longitudinal light curves are presented in Section 5.5.

5.1 Climate on Earth-like planets

The climate of a planet is highly compelled by its global radiative budget. The incoming stellar energy is partially absorbed and balanced by the emitted thermal energy. The latitudinal insolation gradient produces an energy gain in the tropics and a deficit in the poles, and this temperature gradient becomes the primary mechanism of the general circulation of the atmosphere, playing a key role over the climatic conditions and the thermal radiation of the planet. In equilibrium, the net radiative flux at the top of the atmosphere (TOA) across a latitude belt can be written as (Stone, 1978):

$$\frac{dF}{d\phi} = 2\pi R^2 (\cos\phi) \left[Q_\phi (1 - A_\phi) - F_\phi^{IR} \right] \tag{5.1}$$

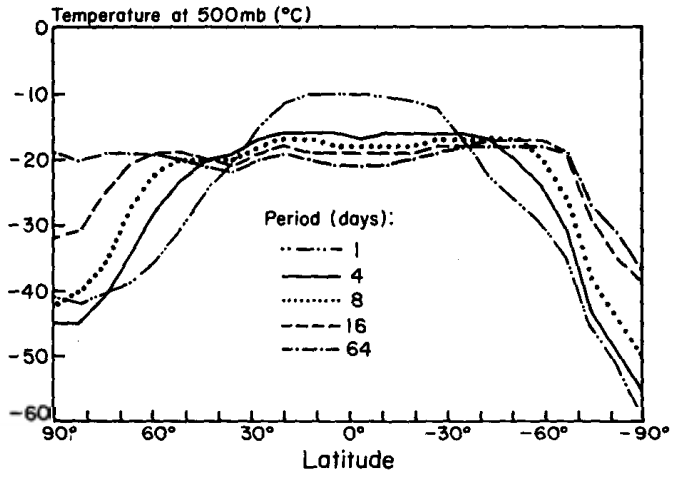

Figure 5.1 Latitudinal profiles of zonal mean 500 mb temperature at rotation periods of 1, 4, 8, 16, and 64 terrestrial days (adapted from del Genio & Suozzo (1987)). The meridional temperature gradient decreases with longer rotation periods.

where ϕ is latitude, R is the planet radius, Q_ϕ is the mean incident stellar radiation per unit area at latitude ϕ, A_ϕ is the mean albedo at latitude ϕ and F_ϕ^{IR} is the mean thermal emitted flux per unit area at latitude ϕ. In order to balance this temperature gradient, a meridional energy transport is stablished, forming the Hadley cell, which constitutes a fundamental feature of the planetary circulation. The influence of the physical characteristics of the planet (the rotation rate, the orbital parameters, the albedo or the global temperature) on the Hadley cell and its effects over the planetary climate has been studied by numerous authors:

Influence of the rotation rate.– The heat flux is related to the planetary rotation rate as a function of $(\partial\theta/\partial y)^2/f^2$, where $(\partial\theta/\partial y)$ is the local meridional temperature gradient, $f = 2\Omega\sin\phi$ is the Coriolis parameter, Ω is the angular velocity of the planet and ϕ is the latitude (Stone, 1972). The latitudinal temperature gradient is greater with faster rotation, the turbulence created by the Coriolis effect implies less efficiency on the meridional heat transport and, as a consequence the planet has warmer and wetter tropics and

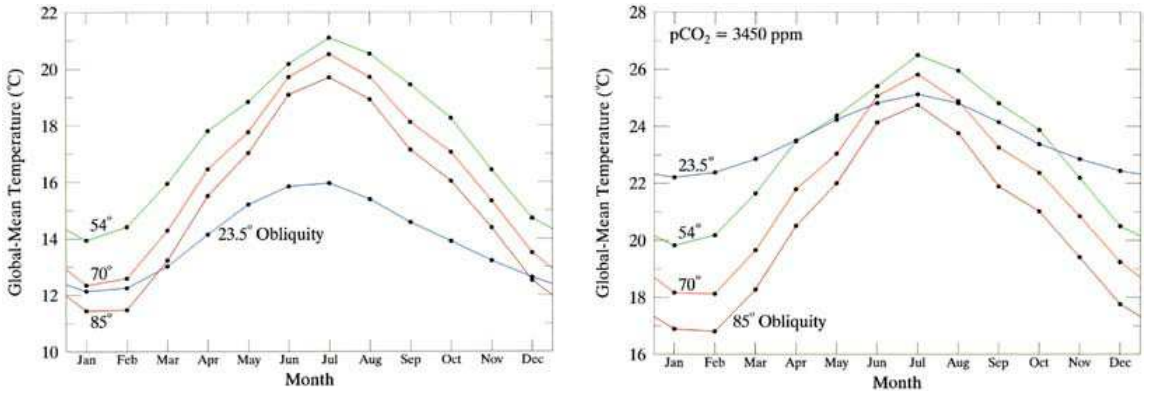

Figure 5.2 Global mean surface temperature for the present Earth (*left*) and the Earth with a high concentration of CO_2 (3450 ppm) (*right*) at planetary obliquities of 23.5° (present Earth), 54°, 70° and 85° (from Williams & Pollard (2003)).

dryer and colder subtropics. Slower rotations, on the contrary, have smaller temperature gradients because the decrease in turbulence makes the meridional heat transport more efficient (Fig. 5.1). Hadley cells are larger with warmer and moister poles and extense arid zones (Hunt, 1979). The regular 3-cell circulation pattern (Fig. 2.8) is replaced by one large Hadley cell and superrotation appears at high altitudes for periods larger than 4 days (del Genio & Suozzo, 1987).

Influence of the obliquity of the rotation axis.– Williams & Pollard (2003) (Fig. 5.2) investigates the effect of obliquity on the Earth climate (for 23.5°, 54°, 70°, and 85° of inclination) under the present conditions of the atmosphere and for high concentrations of CO_2 (3450 ppmv). Large obliquity angles ($\geqslant$54°) give extreme seasonal variations and, because of the continental distribution, the effect is specially amplified during northern summer with temperatures up to 100°C at mid-latitudes. In the case of an atmosphere with a high concentration of CO_2, the planet is globally warmer. The change on the mean surface temperature of the planet respect to the present atmosphere is particularly significant for the present Earth obliquity over higher angles of

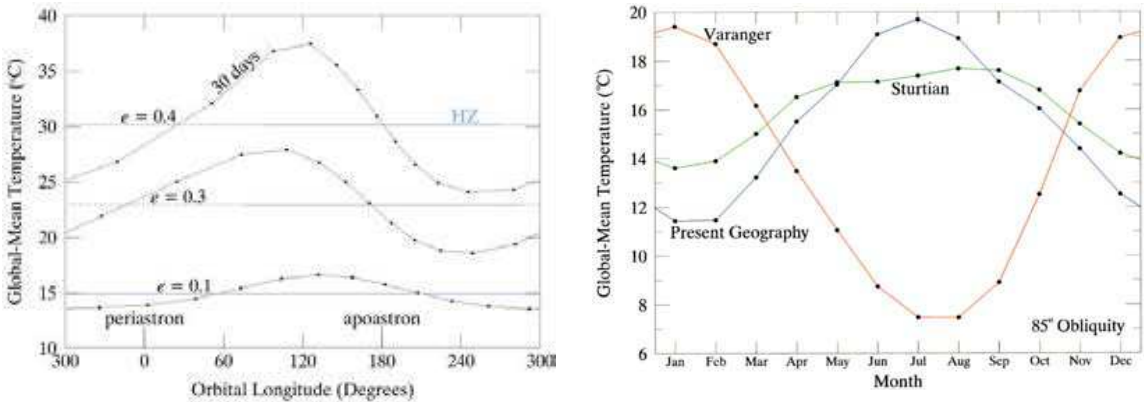

FIGURE 5.3 *Left*: Global mean surface temperature for the present Earth at eccentricities of 0.1, 0.3 and 0.4 (from Williams & Pollard (2002)), the time spent inside the HZ is indicated as a solid blue line. *Right*: Seasonal variation of the global mean surface temperature for three Earth-like planets with an obliquity of 85° and different continental distributions, the present Earth (blue) and the two paleo-climates of the Sturnian glaciation (∼750-720 Ma) with an equatorial ensemble of continents, and the Varanger glaciation (∼610-575 Ma) with a concentration of lands in the South Pole (from Williams & Pollard (2003)).

inclination of the rotation axis. The reason of this temperature increment is that the permanent and the semi-permanent snow-ice cover on the Earth poles is significantly reduced. The global temperature at higher obliquity configurations is less sensitive to an increase of CO_2, because the regions with a permanent snow-ice cover are rare and they have a little contribution to the global temperature of the planet. Although this increment in temperature is important, it is relevant to note that the planet does not turn into a runaway greenhouse (or snowball) state in any case.

Influence of the eccentricity of the orbit.– Williams & Pollard (2002) studies the effect of eccentricity on the habitability of the Earth, by testing the changes for the present Earth at eccentricity values of 0.1, 0.3, and 0.4 (Fig. 5.3

(left)). The time averaged flux $< F >$ over an eccentric orbit is given by:

$$< F > = \frac{L_*}{4\pi R_P^2 \sqrt{1-e^2}} \tag{5.2}$$

where L_* is the stellar luminosity and e is the eccentricity. Thus, at higher eccentricities, the global mean surface temperature rises. For an Earth-analogue at e=0.4, the global temperature is 15° higher, the seasonal variation is also more intense and these conditions lead to severe climates. However, the planet keeps liquid water on the surface in all the cases of the study.

Global warming impact.– An increment in the global temperature produces a tropospheric lifting and a greater static stability of the subtropics (Frierson et al., 2007). Consequently, the Hadley cell expands to higher latitudes, the jet streams and the storm tracks move poleward, the polar vortex is intensified and precipitation and moisture decrease in the subtropics (Lu et al., 2007). As a result, the subtropical regions are drier and extend to higher latitudes than on the present Earth, and therefore the planet has an extreme climate (Solomon et al., 2007).

Continental effects.– The presence of continental lands strengthens the Hadley cell transport during winter and weakens it during summer (Greene, 1998). The increase in surface friction and the development of strong monsoons are the sources of this behavior. In the case of the Earth, because of the predominance of continents on the Northern Hemisphere, they produce lower temperatures during the northern winter (NW) and higher temperatures during the northern summer (NSu) than in the absence of continents (Cook, 2003). Williams & Pollard (2003) studies three continental distributions: the present Earth, a south polar continent, similar to the Varanger glaciation (∼610-575 Ma) configuration, and an equatorial continent that corresponds to the conformation during the time of the Sturtian glaciation (∼750-720 Ma). At an obliquity of 85°, the equatorial distribution shows the mildest seasonal variation of surface temperature (∼4°), whereas the polar continental configuration suffers the most

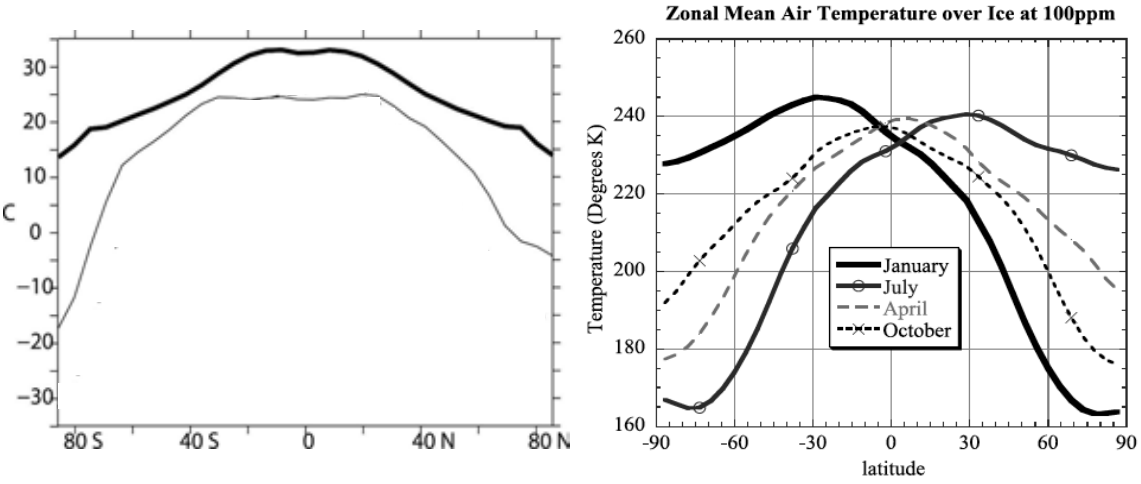

Figure 5.4 *Left*: Annual zonal average air surface temperature (°C) for an aquaplanet (thick solid), the present Earth (thin solid) (adapted from Smith et al. (2006)). *Right*: Seasonal cycle of the snowball zonal mean air temperature over the ice at a 100 ppm CO_2 concentration (from Pierrehumbert (2005)).

acute, with a change of ∼12° between the southern summer (SSu) and the southern winter (SW) (Fig. 5.3, right). In this case, the effect is amplified by the fact that the planet is near periastron – receiving a larger amount of stellar radiation– during the southern summer, and apastron during southern winter. Snow and ice cover the lands of the Varanger planet but the ocean is just covered on ice in certain areas near the coast.

Aquaplanets.– Water worlds have been proposed as possible bodies in the Habitability Zone (HZ) (Léger et al., 2003, 2004; Sotin et al., 2007). On an aquaplanet, the surface is covered by a 50 m deep slab ocean, in the absence of continents, which add surface friction and distort wind currents, the atmospheric circulation of this type of planets differs greatly from the circulation found on Earth. The distribution of the temperature field (Fig. 5.4, left) is essentially zonal (Smith et al., 2006) with a slight hemispherical asymmetry due the eccentricity of Earth's orbit, because of a higher insolation during the

SSu than during the NSu. Although the wind field is also zonal with jets both in the atmosphere and the ocean, the meridional heat transport is very effective, favored by the ocean Ekman transport on the subtropics that causes a meridional transport of water, and the eddy-driven subduction, that allows the exchange of water masses between the ocean surface and its interior (Smith et al., 2006; Marshall et al., 2007; Codron, 2012). The annual mean surface temperature of an Earth-like aquaplanet is 300 K, with a temperature gradient from 286 K on the poles to 306 K on the subtropics. The polar ice has a great influence on the climate as it increases the planetary albedo and at the same time absorbs a certain amount of heat that it is driven poleward in order to maintain equilibrium. The polar ice caps on the Earth-like aquaplanet reach $\sim 55^{\circ}$ latitude (Marshall et al., 2007). Smith et al. (2006) and Enderton & Marshall (2009) showed that continental barriers prevent the formation of polar ice caps.

Snowball planets.– The snowball Earth hypothesis sets that the planet surface became entirely frozen ("hard snowball" state) or nearly entirely frozen ("slush snowball" state) more than 650 Ma ago. This state might have been produced by several factors such as a decrease of the stellar energy, perturbations in the planetary orbit, a reduction of the atmospheric concentration of greenhouse gases or an increment in the volcanic activity. Any of these circumstances can derive in an initial cooling of the planet that would lead to a snowball state. The ice cover increases the global albedo, lowering the temperature of the planet and reinforcing the creation of ice and snow in a positive feedback. Because of the low concentration of water vapor in the atmosphere, surface temperatures drop below 170 K with a maximum temperature of 240 K, which 30 degrees below deglaciation, for the hard snowball (Fig. 5.4, right) (Pierrehumbert, 2005). Although in general a decrease in the stellar radiation or a decrease in the concentration of greenhouse gases can produce a snowball state, the planet remains globally iced despite an increase of solar energy to a present solar constant – in case the agent of glaciation was

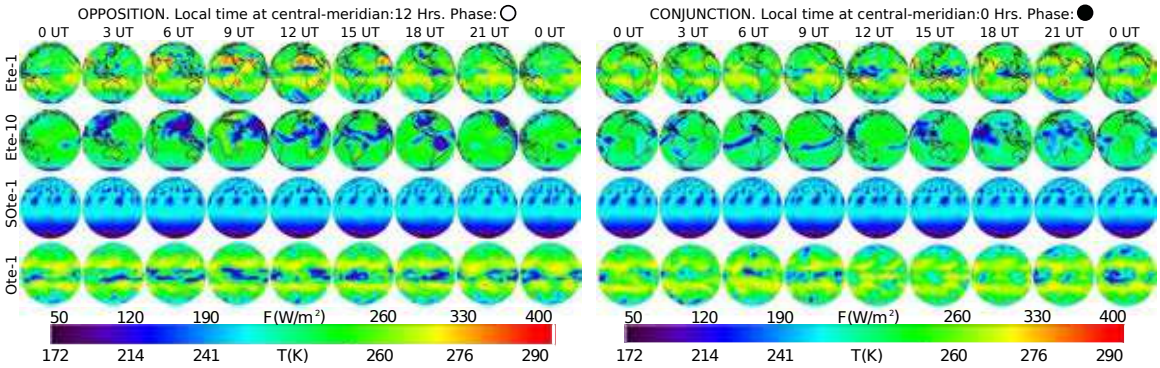

FIGURE 5.5 TOA-all-sky flux/brightness temperature towards an observer at opposition (left) and conjunction (right) during one rotation (UT time) at northern summer for the terrestrial planets (from top to bottom) Ete–1, Ete–10, SOte–1, and Ote–1.

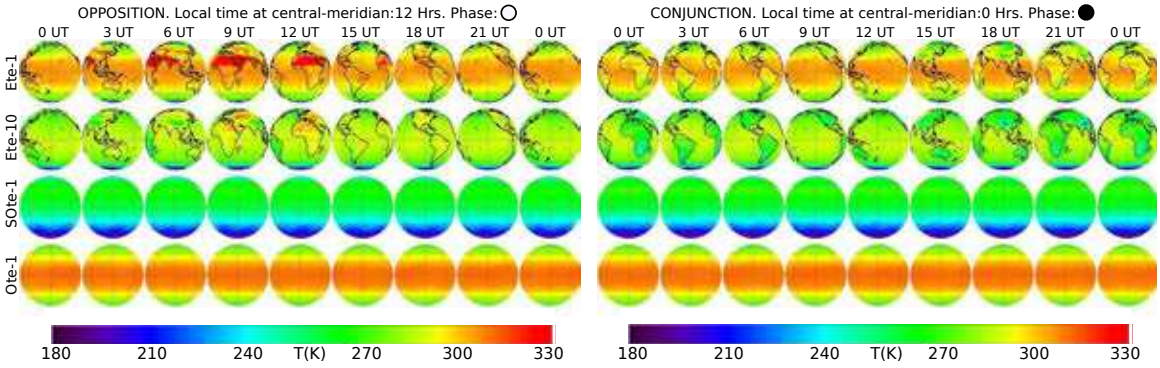

FIGURE 5.6 Surface temperature towards an observer at opposition (left) and conjunction (right) during one rotation (UT time) at northern summer for the terrestrial planets (from top to bottom) Ete–1, Ete–10, SOte–1, and Ote–1.

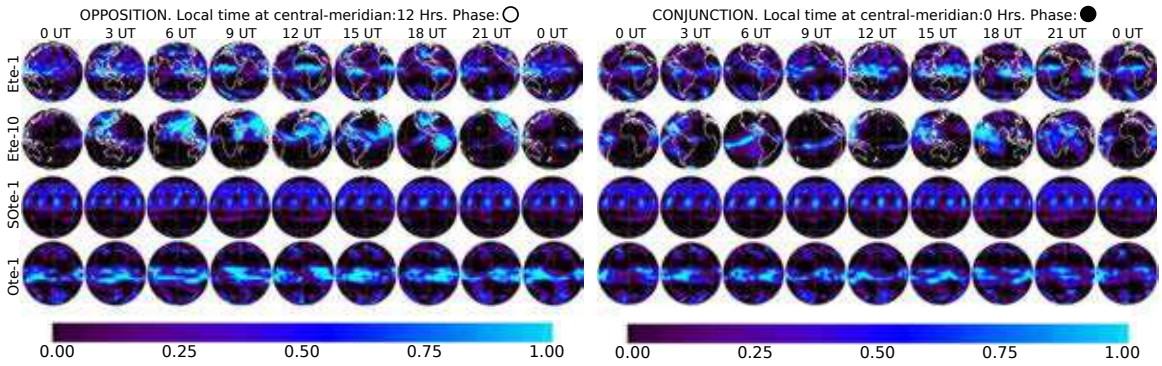

FIGURE 5.7 High cloud fraction for an observer at opposition (left) and conjunction (right) during one rotation (UT time) at northern summer for the terrestrial planets (from top to bottom) Ete–1, Ete–10, Ote–1, and SOte–1.

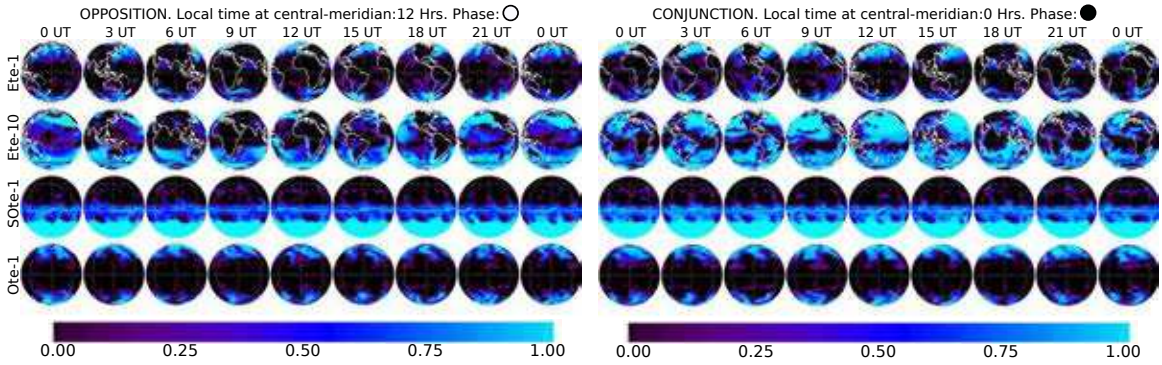

FIGURE 5.8 Low cloud fraction for an observer at opposition (left) and conjunction (right) during one rotation (UT time) at northern summer for the terrestrial planets (from top to bottom) Ete–1, Ete–10, Ote–1, and SOte–1.

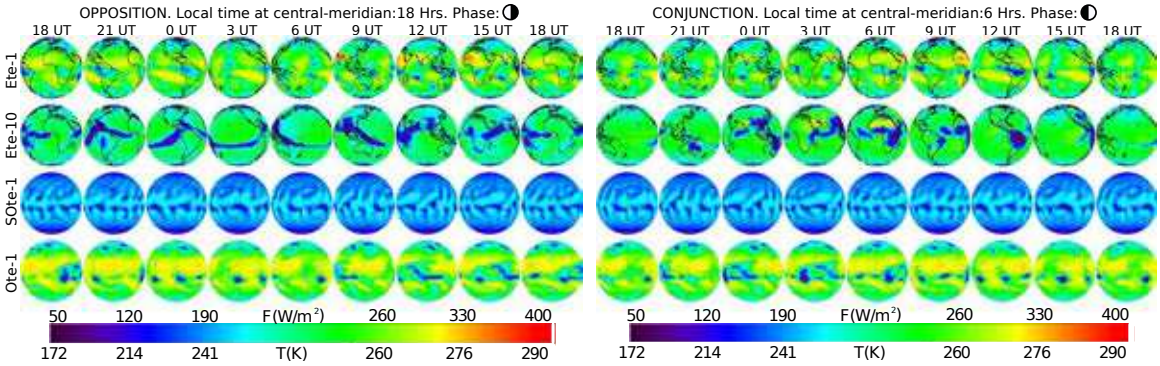

FIGURE 5.9 TOA-all-sky flux/brightness temperature towards an observer at opposition (left) and conjunction (right) during one rotation (UT time) at northern spring for the terrestrial planets (from top to bottom) Ete–1, Ete–10, SOte–1, and Ote–1.

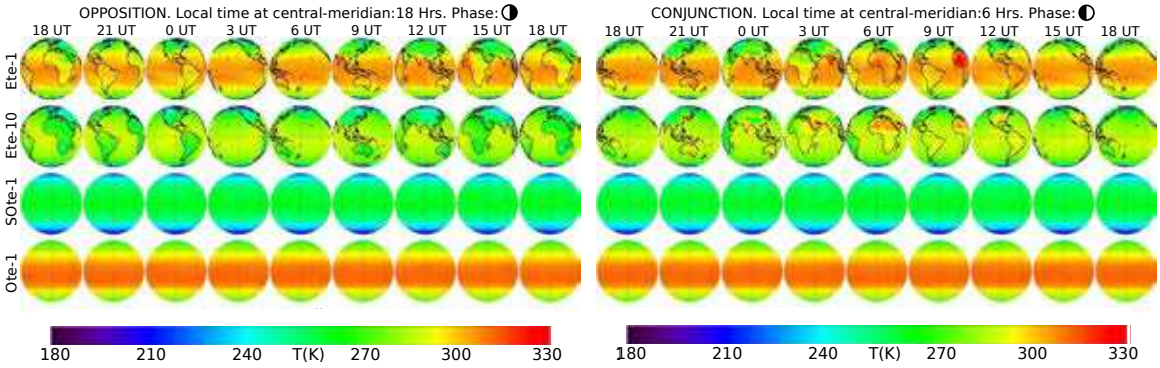

FIGURE 5.10 Surface temperature towards an observer at opposition (left) and conjunction (right) during one rotation (UT time) at northern spring for the terrestrial planets (from top to bottom) Ete–1, Ete–10, SOte–1, and Ote–1.

Table 5.1. Planetary specifics

	Rotation period (sidereal days)	Type of planet
Ete–1	1	Earth-like
Ete–10	10	Earth-like
Ote–1	1	Aquaplanet
SOte–1	1	Snowball Aquaplanet

Note. — **Notation**: *E*–earth-like, *O*–ocean planet, *S*–snowball, *t*–tilted, *e*–Earth's eccentricity, –(rotation period); i.e. *Ete-1* corresponds to the Earth. All the planets have Earth's orbital configuration: obliquity= 23.44°and eccentricity= 0.0167.

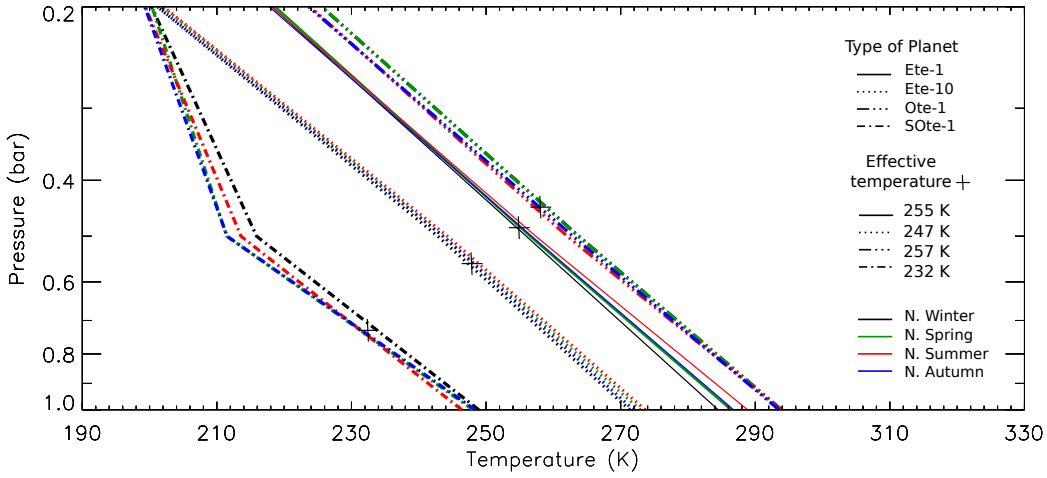

Figure 5.11 Atmospheric profiles for Ete–1, Ete–10, Ote–1, and SOte–1. Colours correspond to different points on the orbit, representing northern hemisphere seasons: winter (black), spring (green), summer (red), and autumn (blue).

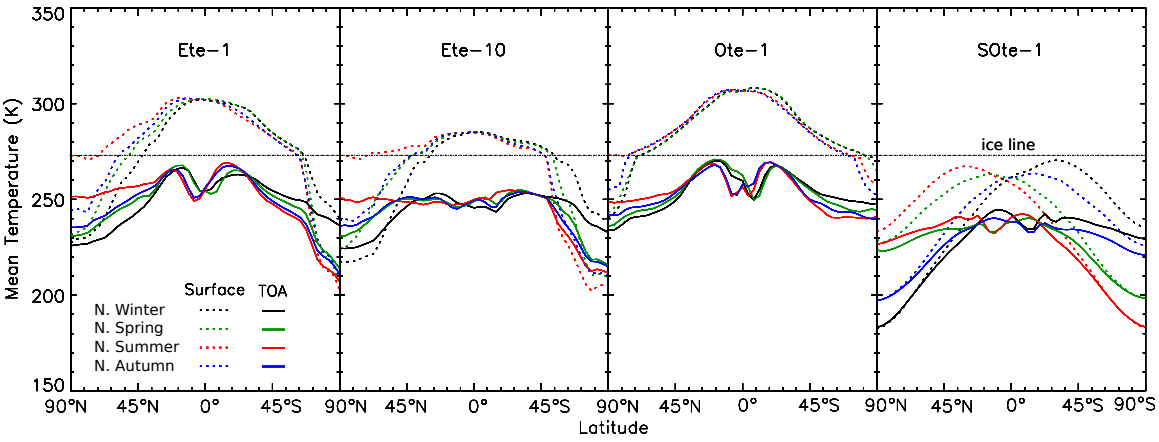

Figure 5.12 Mean temperature vs latitude at surface (dotted) and TOA brightness temperature vs latitude (solid) for the terrestrial planets Ete–1, Ete–10, Ote–1, and SOte–1. Colours represent orbital fraction and the corresponding seasons in the northern hemisphere: winter (black), spring (green), summer (red), and autumn (blue).

a decrease in the stellar energy–, or despite of a CO_2 concentration change to ∼10 times the present atmospheric level (PAL) (3480 *ppmv*). However, ice melting is produced at CO_2 concentrations of ∼100 PAL and result in lower fractions of ice covering than present Earth (Marotzke & Botzet, 2007).

5.1.1 Data

In this study, we have used LMDZ GCM data (Section 3.2) to build four different planets varying the rotation rate (1 or 10 days) and the planetary surface (Table 5.1). All the planets have the atmospheric composition, the axial tilt and the orbital configuration of the Earth. We have reproduced the Earth (Ete–1), in order to validate the application of the data. Then, we have built an Earth-like planet with a rotation period of 10 days (Ete–10), an Earth-like aquaplanet (Ote–1) and a hard-snowball aquaplanet (SOte–1) on which the solar constant has been diminished to 80% in order to achieve the snowball state.

Table 5.2. Global parameters of radiation

	T_{eff} [a](K)	A	CRF (W/m^2)	g_N	T_S(K)
Ete–1	255	0.30	-27.2	0.39	287
Ete–10	248	0.37	-27.5	0.31	272
Ote–1	258	0.26	-28.7	0.41	294
SOte–1	233	0.51	-16.7	0.22	248

Note. — The effective temperature T_{eff}, Bond albedo A, normalized greenhouse parameter g_N, cloud radiative forcing CRF and surface temperature T_S are determined according to the calculations shown in Section 2.2.

[a]The temperature uncertainty is $\pm 5{\cdot}10^{-4}K$, the precisions shown in the table are chosen for simplicity.

Table 5.3. Characteristics of the Troposphere[a]

	H (km)	N (σ_N) ($10^{-5}s^{-1}$)	L (σ_L) (10^{-3})	l (σ_l) (km)	a (σ_a) (K/km)	Δ_T	Ro_T
Ete–1	8.402	1250 (30)	238 (3)	1520 (20)	5.9 (0.6)	0.229	0.02
Ete–10	7.970	1300 (20)	746 (7)	4760 (40)	5.9 (0.6)	0.181	1.79
Ote–1	8.594	1230 (30)	239 (3)	1520 (20)	5.9 (0.2)	0.131	0.01
SOte–1	7.224	1140 (60)	211 (6)	1350 (20)	6.5 (0.2)	0.157	0.01

Note. — Stratification vs Rotation: H is the scale height, N is the Brunt-Väisälä frequency, L is the normal Rossby deformation radius, l is the Rossby deformation radius, a is the tropospheric lapse rate, Δ_T is the non-dimensional meridional temperature gradient, and Ro_T is the thermal Rossby radius (calculations according to Section 2.2.3).

[a]The values are restricted to the tropospheric pressure levels of each planet (Fig. 5.11).

5.2 Planetary characteristics

With the purpose of doing the comparative study the climate of these four planets, we have derived certain parameters from the planetary emission maps. Those parameters, presented in Section 2.2, are: the mean effective temperature T_{eff}, the Bond albedo A, the greenhouse parameter g, the mean surface temperature T_S, the cloud radiative forcing CRF, and the Rossby deformation radius l_R. The results are shown in Table 5.2 and Table 5.3. Figure 5.11 presents the atmospheric profiles of each planet and Figure 5.12 shows the mean surface temperature and the mean brightness temperature as functions of latitude for each season.

5.2.1 The Earth

The results of the global parameters of the planet (Table 5.2) are in agreement with satellite observations (Trenberth et al., 2009). The tropospheric profile (Fig. 5.11) shows the predominance of the planet northern hemisphere, warmer during northern summer and colder during northern winter although they correspond to the apastron and periastron positions respectively. This effect is given by the asymmetric distribution of the continental masses on the planet (Chapter 4, Gómez-Leal et al. 2012), and the surface temperature varies from 285-290 K with seasons.

The subtropical regions, where the circulation is driven by the Hadley cells and represented by the flat central zone of the surface temperature meridional gradient (STMG) (Fig. 5.11, dash), extend to $\sim$30° in latitude in both hemispheres and have a mean temperature of $\sim$300 K. The ice layer reaches $\sim$45°N during northern winter, and becomes a half-iced cap at $\sim$10°N during summer. In the South, the permanent polar cap of the Antarctica extends to $\sim$60°S. The polar surface temperatures vary from 230-270 K in the North and 200-240 K in the South.

At mid-latitudes, there is an asymmetry in the meridional surface temperature of both hemispheres. This difference in temperature is the result of the uneven distribution of land on Earth. The predominance of oceans in the southern hemisphere

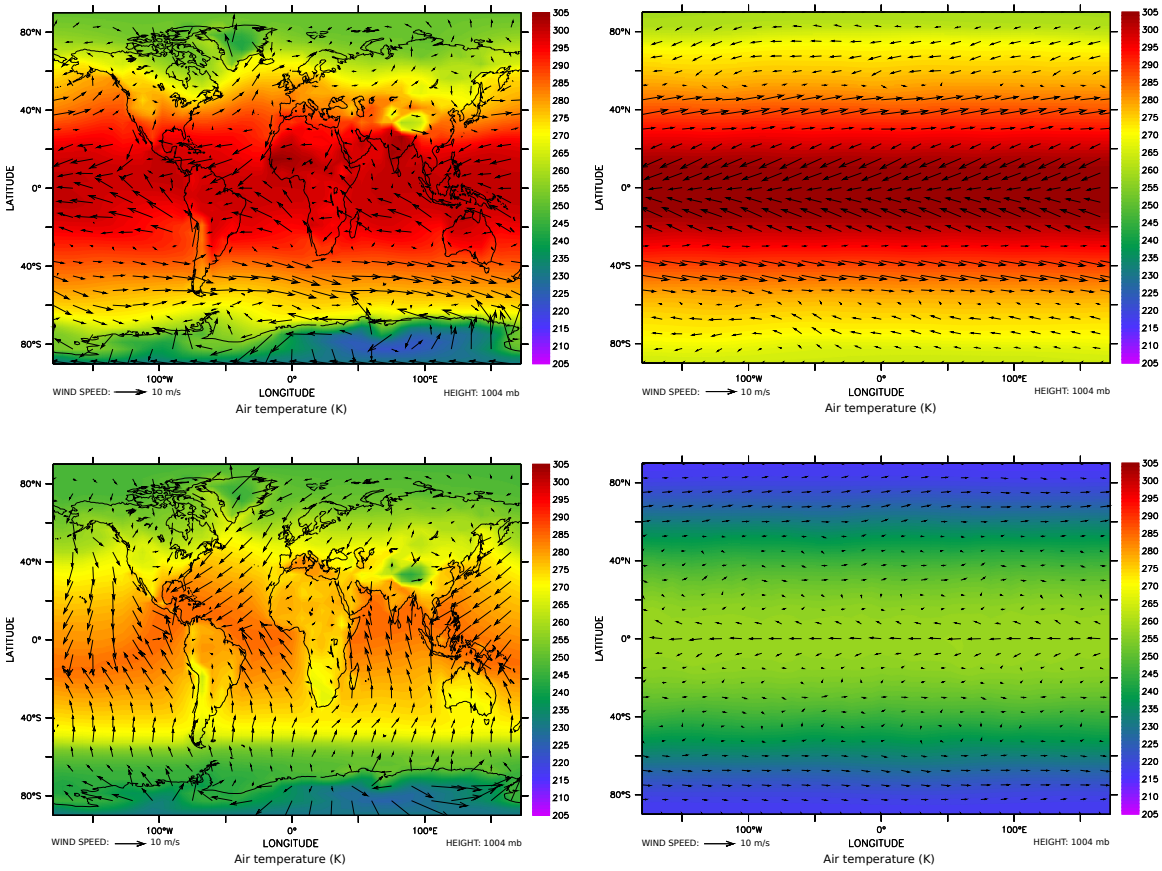

FIGURE 5.13 Mean surface temperature and mean surface wind field for Ete–1 (top-left), Ote–1 (top-right), Ete–10 (bottom-left) and SOte–1 (bottom-right).

produces a small seasonal variation in surface temperature due to the high thermal inertia of water. In contrast, the large continental masses in the northern hemisphere produce a larger variation because in general the emissivity of bare land (summer) is higher than the emissivity of water, whereas the emissivity of snow (winter) is lower.

The brightness temperature meridional gradient (BTMG) (Fig. 5.11, solid) decreases near the Equator, because of the absorption of convection clouds that condense over the Intertropical Convergence Zone (ITCZ). The ITCZ moves from one side to the Equator to the other, following the latitudinal change of the ecliptic

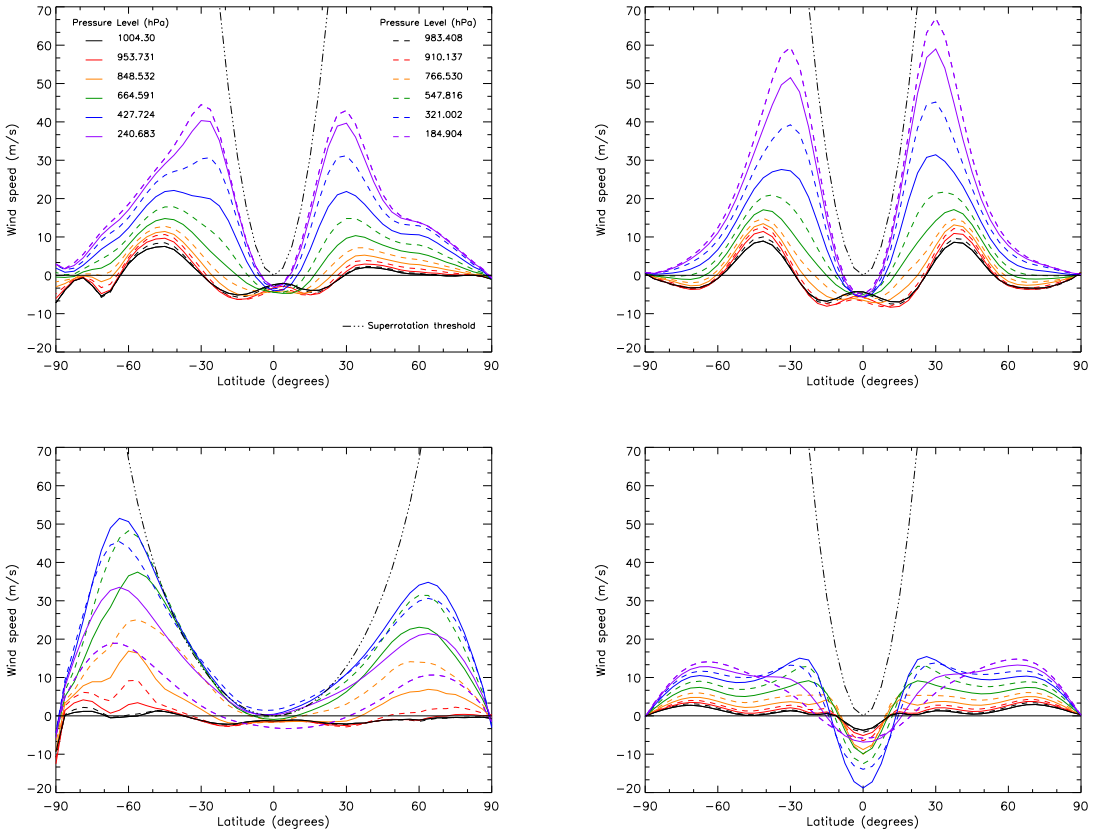

Figure 5.14 Mean zonal annual wind for the tropospheric levels of Ete–1 (top-left), Ote–1 (top-right), Ete–10 (bottom-left), and SOte–1 (bottom-right). Superrotating winds lie above the wind speed limit u_L(dash-dot black line), described in Section 2.2.3.

with seasons. The absorption is more relevant in the northern hemisphere, as the result of the continental distribution: the seasonal shifts of the ITCZ and the great seasonal temperature and humidity differences between the continent and the ocean create monsoons, which are particularly important on India and Indonesia (Philander et al., 1996). Figure 5.5 (northern summer) and Figure 5.9 (northern spring) show the TOA-emission flux of the Earth (Ete–1). We can distinguish the ITCZ clouds, the temperature differences between the subtropical regions and the rest of the planet, and the diurnal cycle of the arid zones, especially on the Sahara desert. There is

a large fraction of high clouds in the planet (Fig. 5.7), the clouds along the ITCZ have two stable zones, one over Indonesia and the other over the african equatorial savanna, whereas low clouds condense over the cold polar oceans (Fig. 5.8).

Figure 5.13 (top-left) shows the patterns of the mean horizontal surface wind field, with the convergence at the convection region of the ITCZ at the Equator, where the Hadley cells of each hemisphere meet and specially the convergence of winds over Indonesia, because of the coincidence of the Hadley and the Walker cells (a circulation over the Pacific ocean). The results of Earth's tropospheric parameters (Table 5.3) are in agreement with the literature (e.g., Mitchell & Vallis 2010). Figure 5.14 illustrates the zonal wind speed at several pressure levels of the troposphere. The figure shows that Earth zonal winds are outside the region of superrotation, where the speed is higher that the rotation of the solid body (region inside the black dot-dash-line), and the planet does not present superrotation by any of the criteria of Section 2.2.3, u$<$ u$_L$, Ro$_T$ $<$ 1.3 (Mitchell & Vallis, 2010), and L$_R$ $<$ 1 (del Genio & Suozzo, 1987) (Table 5.3). The Southern Hemisphere shows higher wind velocities than the Northern Hemisphere because of a greater latitudinal temperature gradient ($U_T \sim T_S \Delta_T$, from Eq. 2.14).

5.2.2 The slow Earth

In order to study the effects of the rotation period over the climate, we have study the case of an Earth with a rotation period of 10 days. Because of the weaker Coriolis force, the meridional transport is very effective and the global climate is colder (Fig. 5.11). The Hadley cells extend to higher latitudes with colder subtropical temperatures (Fig. 5.12). In summary, Ete–10 has lower mean surface temperature (272 K) and effective temperature (248 K), slower zonal winds, a diurnal convection cloud formation cycle over the continents and a thick layer of low clouds over the oceans (Fig. 5.8). As a consequence of the cold surface temperature (maximum$\sim$280 K), the seasonal variability is lower than on Earth.

The incoming stellar radiation is largely reflected by low clouds (high albedo), cooling the planet, and as a result a vast part of the surface is frozen (δ_{ice} $\geq$40° latitude). Convection clouds are formed along the ITCZ, which in this case is modified by the dominant meridional winds (Fig. 5.13).

It is interesting to note that as a consequence of the temperature contrast between the continental land and the ocean (Figs. 5.5 and 5.6), convection clouds also condense over large continental regions, in this case as massive monsoons. The absorption of light produced by these clouds is the cause of the general decrease in the brightness temperature along the subtropical regions (Fig. 5.12). The diurnal cycle influence the condensation of high clouds, which is increases during the afternoon. During summer, the cloud cover of the asian monsoon extends from Papua to half of Siberia (Fig. 5.7) and another monsoon covers America with the only exception of the Southern Cone.

Figure 5.13 (bottom-left) shows the predominance of the meridional component of the horizontal wind field and the modification of the ITCZ. The scale height H and the Brunt–Väisäla frequency N are modified by temperature (Table 5.3), whereas the Rossby deformation radius is determined by the rotation rate Ω_r. As on Earth, the distribution of the continents also determine the wind circulation, but here the surface winds are slower due to the low temperatures. Figure 5.14 (bottom-left) shows that there is a faint equatorial superrotation regime at the upper levels of the troposphere, confirmed by a value of the thermal Rossby number greater than 1.3 (Ro_T= 1.79). However, the criteria of a L_R >1 for a superrotation regime differs with the results (L_R= 0.746).

5.2.3 The Earth-like aquaplanet

In the absence of continents, the atmospheric circulation of an aquaplanet such as Ote–1 is less complex than in the case of terrestrial planets: The meridional gradient of the stellar insolation determines the temperature of the planet and its distribution.

The large surface specific humidity of the planet (50% higher than Earth's levels, Kalnay et al. 1996) favors the production of high clouds, the greenhouse effect is larger (Table 5.2) than on Earth, and as a consequence, the aquaplanet analogue has a warmer global surface temperature (Fig. 5.11).

The seasonal temperature variation in the highest part of the troposphere is given by the change in high cloud fraction, whereas the surface temperature does not vary considerably because of the large thermal inertia of water. The subtropical surface temperature rises to 310 K, the polar caps melt in summer, in winter (Fig. 5.12) the North Pole have a surface temperature of ∼240 K, whereas the South Pole winter reaches ∼260 K. We can see the effect of the eccentricity of the orbit, as the southern summer (at periastron) is slightly warmer than the northern one (at apastron). Figures 5.5 and 5.6 show the temperature dependence with latitude, with a large extension of the cloudy ITCZ and formation of low clouds over the polar regions.

The planet has a zonal wind pattern analogous to Earth without superrotation, and a similar tropospheric parameters (Table 5.3). However, in this case the higher wind speeds are in the Northern Hemisphere (Fig. 5.14) and have a different origin, because of the eccentricity of the orbit the mean surface temperature is slightly higher in the tropics during the southern summer (Fig. 5.12, black dash line), and specially in the south pole where the ice cap almost disappears, at the same time a large temperature gradient is created in the northern hemisphere ($U_T \sim T_S \Delta_T$) to maintain equilibrium, and then the north polar ice cap increases, reaching ∼70 degrees in latitude. As a result, winter surface temperatures are more severe at the North Pole than at the South Pole (red dash line).

5.2.4 The Snowball aquaplanet

In the case of the snowball planet SOte–1, the surface is completely frozen; with a mean surface temperature of 248 K (∼40 degrees colder than the Earth). The snow

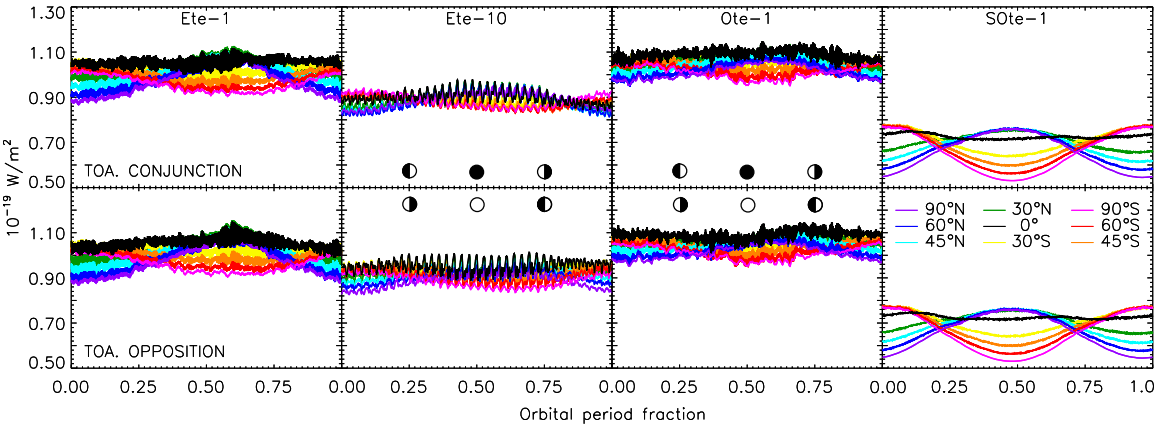

FIGURE 5.15 TOA-all-sky flux orbital series for the terrestrial planets Ete–1, Ete–10, Ote–1, and SOte–1, for an observer at conjunction (top row) and at opposition (bottom row). The circles indicate the illumination phase of the planet for an observer at the ecliptic plane.

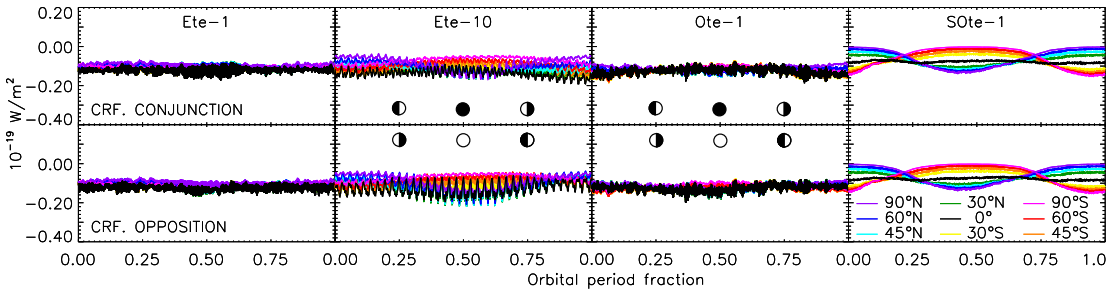

FIGURE 5.16 Corresponding cloud radiative forcing (CRF) for the terrestrial planets Ete–1, Ete–10, Ote–1, and SOte–1 during one orbit for an observer at conjunction (top row) and at opposition (bottom row). The circles indicate the illumination phase of the planet for an observer at the ecliptic plane.

and the high production of low clouds increase the planetary albedo (Table 5.2). The effective temperature is ∼233 K and the troposphere is constricted to higher pressure levels (∼0.7 bar) (Fig. 5.11). As in the aquaplanes, being at periastron the Southern summer is warmer, with an annual mean surface temperature of ∼270 K

in the regions that are most exposed to solar radiation (Fig. 5.12). Because of the general cold temperatures of the planet, zonal winds are very slow, and the poles are dry and very cold (180-240 K). The rate of cooling of a rising saturated parcel of air depends on the moisture content of the air, and then since cold air has less moisture content, the lapse rate a is higher than in the rest of planets (Fig. 5.11 and Table 5.3).

During winter the whole hemisphere is covered by a thick homogeneous layer of low clouds (Fig. 5.8) and winds are very slow (Fig. 5.14). During summer, there is a condensation of convective clouds mainly near the equator. These clouds are periodically distributed over the surface of the summer hemisphere, because the convective movements are in the scale of the space resolution. High clouds would have a different distribution in a real snowball planet. Taking in account this numerical artifact, the essentials of our results on the planetary characteristics and on the analysis of the signal of the planet do not change. Therefore, we have decided to consider these data in our study. Again because of the low surface temperature gradient, meridional winds are very slow, and the planet does not show superrotation.

5.3 Time series

In this section, we present the analysis of the orbital light curves and the physical parameters that have an influence on the signal. Figure 5.15 represents the orbital thermal light curve of the planet for observers at conjunction and observers at opposition for several inclinations of the planetary view, labeled by the latitude of the sub-observer's point. To study the effect of clouds on the signal, we have calculated the Cloud Radiative Forcing (CRF) (Section 2.2) at any time of observation. Figure 5.16 gives the CRF correspondent to the time series. As the clouds absorb the emission from below, CRF (=$F_{all-sky}$ - F_{clear}) is a negative magnitude. Table 5.4 presents the time series variability. It is also useful to associate the time series with the rotation maps from Figure 5.5 to Figure 5.10.

5.3.1 The Earth (Ete–1)

Comparing the light curves obtained at conjunction and at opposition of Figure 5.15, we do not observe a substantial difference in flux with a change in the planetary phase angle. The signal shows a combination of several effects: the large modulation reprints the seasonal cycle with a predominance of the NH because of the uneven distribution of continents, and the smaller variability is due to the passage of warm regions (Sahara) and cold regions (Indonesia) (Chapter 4) with the rotation of the planet. The cloud production is higher during summer, specially in the NH, due to the temperature increase.

5.3.2 The slow Earth

As in the case of the Earth, the light curve of Ete–10 has also a seasonal and a rotational variation. However, the slow Earth is a colder planet, the rotational modulation due to warm spots is rare. In this case, we can see the rotation of the planet because there is a difference in the emission with the illumination phase of the planet, due to the diurnal cycle of high clouds. The massive condensation of clouds over the continents produce a strong modulation with the rotation of the planet. High clouds condense massively during daylight, absorbing the planetary emission and producing a decrease in brightness temperature. The cloudy regions appear as large cold spots over the continents and the contrast between the clear and the cloudy regions produce the oscillation seen in Figure 5.15. The production of clouds is more important for low latitudes and particularly during northern summer (Fig. 5.16). Being a colder planet, the orbital variability of the Northern Hemisphere is lower than on Earth (Table 5.4) However, the orbital variability of the Southern Hemisphere is similar in both planets because of the predominancy of the oceans, which have a low thermal inertia.

Table 5.4. Time series variability

	Variability	Orbital phase	Latitude								
			90	60	45	30	0	-30	-45	-60	-90
Ete–1	Rotation	[0,1/12]	3	5(4)	6(5)	6(5)	6(4)	5(4)	4(3)	3(3)	2
		[4/12,5/12]	3	4(5)	5(6)	5(7)	4(6)	4(5)	4(5)	3(4)	2
		[7/12,8/12]	3	5(6)	6(8)	7(9)	7(9)	6(7)	5(5)	3(4)	2
		[10/12,11/12]	3	6(5)	6(6)	7(6)	6(5)	5(4)	4(4)	3(3)	2
	Orbit	[0-1]	19	17(15)	14(12)	11(9)	5(3)	4(6)	6(8)	8(9)	10
Ete–10	Rotation	[0,1/12]	2	4(3)	4(4)	5(5)	4(6)	4(6)	4(6)	3(5)	3
		[4/12,5/12]	3	6(5)	6(6)	6(7)	7(8)	5(7)	4(6)	3(4)	3
		[7/12,8/12]	4	7(8)	8(9)	9(10)	10(11)	8(9)	6(7)	4(4)	3
		[10/12,11/12]	3	6(4)	6(5)	7(6)	6(7)	5(7)	4(6)	3(5)	3
	Orbit	[0-1]	10	11(8)	11(7)	10(5)	6(3)	5(5)	6(6)	8(7)	9
Ote–1	Rotation	[0,1/12]	2	4(3)	4(4)	5(4)	5(4)	5(4)	4(4)	4(3)	2
		[4/12,5/12]	2	4(4)	5(5)	6(6)	6(7)	6(7)	5(6)	4(5)	2
		[7/12,8/12]	1	3(4)	4(5)	5(6)	6(7)	6(7)	5(6)	4(5)	2
		[10/12,11/12]	1	3(4)	4(5)	5(6)	6(7)	5(7)	5(6)	4(5)	2
	Orbit	[0-1]	8	8(6)	8(5)	7(3)	5(4)	5(7)	6(8)	8(9)	9
SOte–1	Rotation	[0,1/12]	2	2(2)	2(2)	1(1)	1(1)	1(1)	1(1)	1(1)	1
		[4/12,5/12]	2	2(2)	2(2)	1(1)	1(1)	2(2)	2(2)	3(3)	3
		[7/12,8/12]	1	1(1)	1(1)	1(1)	1(1)	2(1)	2(2)	2(2)	2
		[10/12,11/12]	3	3(2)	2(2)	2(2)	1(1)	2(2)	2(2)	2(2)	2
	Orbit	[0-1]	33	27(27)	22(21)	14(14)	4(5)	18(19)	25(26)	31(31)	36

Note. — Mean amplitude values of rotational and orbital variability of the time series of the following planets: Earth (Ete–1), slow Earth (Ete–10), aquaplanet analogue (Ote–1), and snowball (SOte–1) at opposition and conjunction (in parentheses) for several sub-observer's point latitudes. Values are calculated as the percentage over the mean value. Rectangles contain latitudes at summer.

5.3.3 The Earth-like aquaplanet

As shown in the previous section, Ote–1 is globally warmer than the Earth. There is a seasonal variation due to insolation change produced by the tilt of the rotation axis. The high thermal inertia of water prevents from having any contrast between day and night (opposition-conjuntion views) and the presence of clouds is the only factor that produces the rotation variability of the signal. The CRF is slightly larger during the summer noon.

5.3.4 The Snowball aquaplanet

During winter, as the atmosphere is very cold, dry, with little circulation and low clouds cover the surface, the surface emission is not significantly disturbed and the thermal light curve strongly depends on the inclination of observation. However in summer, as the atmosphere becomes warmer, the circulation of the atmosphere is enhanced, convective clouds are produced and then the whole hemisphere has similar brightness temperatures Figure 5.12. The CRF is larger during the southern summer day, as the summer of the southern hemisphere is more extreme because of the eccentricity of the orbit.

5.3.5 Observed parameters

Table 5.5 shows the results for the mean effective temperature and the albedo for an observer at opposition and at conjunction (in parentheses) at several sub-observer latitudes. Perspective favors the brightness temperatures near of the sub-observer point. for that reason low latitudes show warmer temperatures than the global mean, high latitudes have colder values, and mid-latitudes ($\sim 30^\circ$) being more temperate, have similar values to the global mean.

On the slow Earth, despite the large modulation due to convection clouds, the mean effective temperature is higher than the global value for an observer at opposition (who sees the winter–night and summer–day), whereas at conjunction

Table 5.5. Observed parameters

		Global	Latitude								
		Value	90	60	45	30	0	-30	-45	-60	-90
Ete–1	T_{eff} (K)	255	252	253	254	256	257	256	254	253	252
	Albedo	0.29	0.33	0.32	0.30	0.28	0.27	0.29	0.30	0.32	0.33
	$\mathcal{T}$(days)	0.99	1.00	1.00	1.00	1.00	1.00	1.00	1.00	1.00	0.63
Ete–10	T_{eff} (K)	248	247	(246) 248	(246) 249	(247) 250	(247) 251	(247) 250	(246) 249	(246) 248	246
	Albedo	0.37	0.38	(0.38) 0.37	(0.39) 0.36	(0.38) 0.35	(0.37) 0.33	(0.38) 0.35	(0.39) 0.36	(0.39) 0.37	0.38
	$\mathcal{T}$(days)	9.997	10.00	10.00	10.00	10.00	10.00	10.00	9.88	10.00	9.88
Ote–1	T_{eff} (K)	258	255	256	257	258	260	258	257	256	255
	Albedo	0.26	0.30	0.29	0.27	0.26	0.24	0.26	0.27	0.29	0.33
	$\mathcal{T}$(days)	0.997	0.63	1.00	1.00	1.00	1.00	1.00	1.00	1.00	0.63
SOte–1	T_{eff} (K)	233	229	230	232	233	235	233	231	230	228
	Albedo	0.51	0.54	0.53	0.52	0.50	0.49	0.50	0.52	0.53	0.54
	$\mathcal{T}$(days)	0.997	0.63	1.00	1.00	1.00	1.00	1.00	0.88	0.63	0.63

Note. — Observed parameters from the time series: effective temperature T_{eff} (Eq.2.11), albedo (Eq.2.12) and rotational period $\mathcal{T}$ (Eq.2.20) for the planets Ete–1, Ete–10, Ote–1, and SOte–1 at opposition and at conjunction (in parentheses) for several sub-observer's point latitudes. Values are calculated as the percentage over the mean value.

(where the observer sees the winter-day and the summer-night) the values are lower than the global mean, because for a planet with a continental distribution similar to the Earth, the influence of continents prevails over the eccentricity effect (see Table 5.5 and Figure 5.15). Both hemispheres have the same mean effective temperature by latitude but the variability is higher for the NH, where the continental masses are larger. This implies that the northern hemisphere is both warmer and colder than the southern one. As albedo is derived from the effective temperature (Equation 2.9), a lower effective temperature imply higher albedos, which agrees with the fact that an observer at conjunction (who sees the summer-night) sees a higher concentration of low clouds that reflect the solar radiation and increase the albedo values (Table 5.5 , in parenthesis).

In Ote-1 and SOte-1, the rotational variability is similar in both hemispheres, the seasonal variability is higher for the Southern Hemisphere due to the eccentricity of the orbit, as the SSu occurs near the periastron, where the planet suffers a higher degree of solar radiation, producing higher global temperatures. At the opposite place of the orbit, the situation is different. In Ote-1, the SW is also warmer, because the planet develops a large polar ice cap during the NW, as we have previously explained. However in SOte-1, SW is slightly colder, as the planet is already cover with ice, heat transport is very low and the temperature is determined by the eccentricity of the orbit.

5.4 Rotational periodicities

In Chapter 4, we have seen how the autocorrelation of the time series can be used to find the periodicities of planet light curves (Pallé et al., 2008; Gómez-Leal et al., 2012). This method is limited by three factors:

i) The number of periods contained in the series.– The average over a large number of periods reduce the uncertainty of the results.

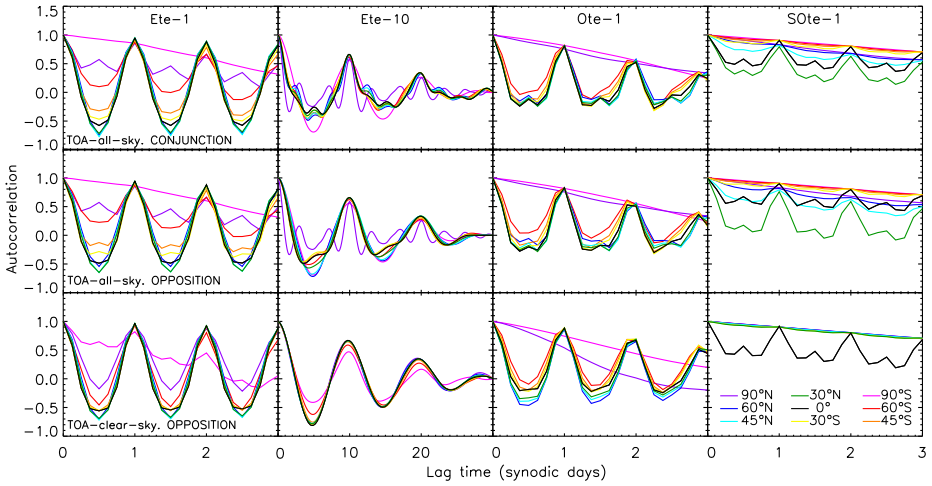

FIGURE 5.17 Autocorrelation series for the terrestrial planets Ete–1, Ete–10, Ote–1, and SOte–1, during northern summer: TOA-all-sky autocorrelation for an observer at conjunction (top), at opposition (middle), and TOA-clear-sky autocorrelation for an observer at opposition (bottom).

ii) The time resolution.– It is important to have a high time resolution to do a good sampling of the periodicity. If the latter is not a multiple of the time resolution, there is a longitudinal angle phase $\Delta\phi$ between the real and the measured period that is cumulative over time, then the longer the time considered, the worser the autocorrelation.

iii) The climatic effects over the signal.– Climate effects have an influence on the autocorrelation function and are also cumulative: as the seasonal flux variation or the random effect of clouds.

In our case we have made the best compromise between these factors. Table 5.5 presents the values of the autocorrelation series of our set of planets for an observer at opposition and an observer at conjunction (in parentheses), for several sub-observer's latitudes at northern summer and Figure 5.17 shows the corresponding

autocorrelation series of the TOA-all-sky emission at conjunction (top row), at opposition (middle row), and of the TOA-clear-sky emission at opposition (bottom row) for several sub-observer's latitudes during three rotational periods of each planet at northern summer. For most observers the period of the planet is well determined within the uncertainty given by the time resolution, with the exception of the polar views.

The common source of rotation in terrestrial planets is the presence of steady high clouds, whereas transient clouds have the opposite effect, usually distorting the periodicity of the planetary signal. In the case of the Earth, the modulation is created by the succession of warm and cold (cloudy) regions of the planet (Chapter 4, Gómez-Leal et al. (2012)). The signal of the slow-Earth is specially marked by the temperature meridional gradient and the temperature contrast between oceans and lands, although most of the time the planet is entirely covered by clouds (Figure 5.7 and Figure 5.8). The oceanic regions are covered with low clouds that are thin to thermal radiation, and high clouds, thick to infrared emission, are placed over the continents. As a result, although the surface temperature is similar, the TOA emission is distinctly different for each type of surface because it comes from different altitudes in the atmosphere, and then the modulation of the signal is very high. The convection clouds disappear during the night, but as they are related to the topography of the planet, the period is still retrieved by slight difference in thermal emission of oceanic and continental regions (in this case continent regions are warmer (see next section, Fig. 5.7) top chart).

On the aquaplanet, high clouds are primarily distributed along the ITCZ, and clouds are rare but quite stable on the snowball planet, because of the cold temperatures. As cloud lifetimes are longer than the rotation period in both planets, the period can be determined despite of having a homogeneous surface.

However, when in the case that the planetary view is uniform and the temperature contrast between clear and cloudy regions is not significant, the period cannot be

estimated. In the case of the Earth, an observer over the Antarctica is not able to determine the period, as the southern hemisphere is mostly covered by oceans and the cold and cloudy antarctic winter does not show temperature variances along the day. This happens also to observers over the poles of the aquaplanet and the snowball planet, particularly in winter over high latitudes, because of the absence of high clouds (Fig. 5.9).

Figure 5.17 shows the autocorrelation series of the four planets during northern summer. Comparing the two bottom charts ("all" and "clear-sky"), we can retrieve the effect of the clouds. The Earth and the aquaplanet does not present relevant differences and the most relevant distortions occur in Ete–10 and SOte–1. In the slow-Earth, convection clouds, attached to humid regions, have also a certain modulation and the signal is less affected, however for polar views (90°N, violet), they mask the diurnal temperature cycle of the surface. In SOte–1, the periodic signal is unmistakably produced by the clouds, the origin of the rotation period comes from the humidity of the ITCZ (clear-sky TOA emission, black line), we also see that the clouds that produce the autocorrelation are more intense during the day at low latitudes.

In summary, if the clouds have longer life-times than the rotation period, they create the periodic signal and the period is easily retrieved from the autocorrelation. On the contrary if the cloud lifetimes are shorter than the rotation period, the periodic signal cannot be calculated from the autocorrelation. In order to retrieved the period, we need a long observation time to have a large number of rotations contained in the signal.

5.5 Longitudinal light curves

After the determination of the rotation period, the observer can built an average rotation light curve in order to identify warm and cold regions on the planet. The average rotation is built by time-folding the signal. In order to avoid the variation

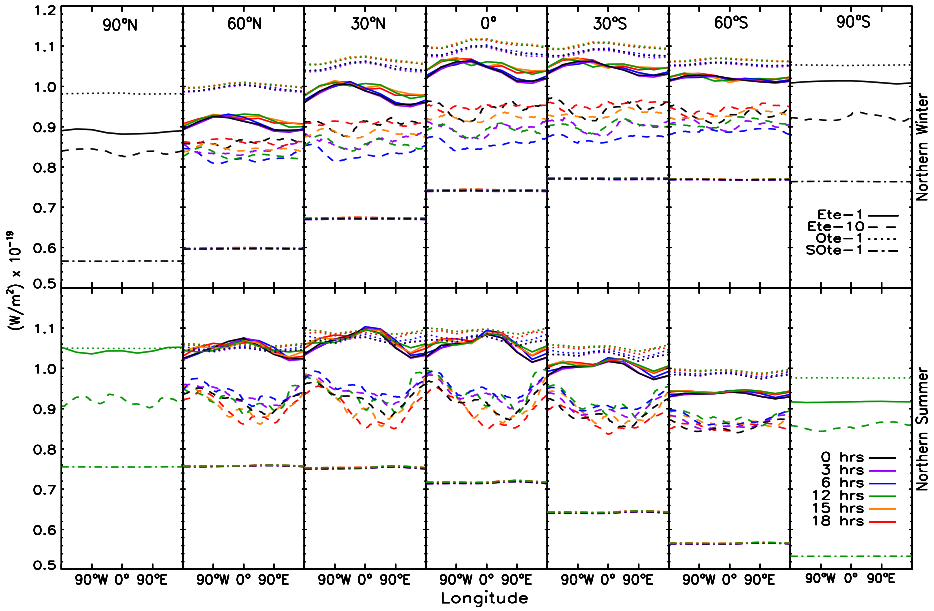

Figure 5.18 Longitudinal light curves: Mean TOA-all sky flux vs longitude, during northern winter (top) and northern summer (bottom) for the latitudes 90°N, 60°N, 30°N, 0°, 30°S, 60°S, and 90°S, colours correspond to local hour at the planetary disk center-meridian towards the observer.

in flux produced by the seasons, and to find a compromise between a good statistics and sampling of the signal, the optimal series length is estimated to be ∼10 days.

Figure 5.18 represents the averaged rotation curve viewed by different observers (sub-observer's latitudes in columns and local hours in colours) for our set of planets during northern winter (top row) and northern summer (bottom row). It is presented as thermal flux in function of the planetary longitude, as it is explained in Section 2.3.2, by this method, we can infer warm and cold regions on the planet. For comparison, the rotational curves of the NASA-SRB Earth are described in Section 4.4. LMDZ results are similar, except for the fact that, although the shape of the graph is the same, the temperature evolution along the day for the maximum (Sahara-Arabian region) and the minima (Indonesia) are not the same, due to the differences in the cloud modeling. However, this fact does not affect the global results

of this study.

There is a diurnal cycle in Ete-10, due to the continental convective clouds that make the planet colder during the evening. These clouds disappear from the view when the Pacific ocean passes through the center meridian, then, as the region is covered with low clouds (Figure 5.7 and Figure 5.8), the global emission is warmer, specially in summer (Table 5.4).

The modulation in Ote–1 is only produced by the regions with a high condensation of clouds. In the snowball planet, the temperature difference between clear and cloudy regions is very low and the effect of clouds is not important. However, the effect of the eccentricity of the orbit is clearly seen, with a warmer summer and a colder winter in the Southern Hemisphere.

5.6 Summary

In this chapter, we have studied the thermal light curves of four Earth-like planets: The Earth; a slow Earth, with a rotation period of 10 days; an aquaplanet with Earth orbital parameters and a snowball version of this aquaplanet. Climate is highly dependent on surface temperature, Bond albedo, rotation rate, cloud covering and continental distribution. Then, we have calculated the global parameters of the atmosphere, discuss the climatic conditions, and study the influence of the physical characteristics of the planet on the signal.

In comparison with Earth's climate, a slow Earth has a colder climate, zonal winds are very slow and the meridional circulation dominates, it also has a diurnal convection cloud formation cycle in the form of huge monsoons and a thick layer of low clouds over the oceans. As a result of a large part of the surface is frozen. Unlike the Earth, there are equatorial superrotating winds in the upper levels of the troposphere.

An aquaplanet analogue has a warmer climate, the greenhouse effect is severe because of the large fraction of high clouds. Surface temperatures of aquaplanets are influenced by the eccentricity of the orbit (the southern summer is warmer because at that moment the planet passes by the periastron).

The snowball climate is cold and dry with very slow winds, a layer of low cloud covers the surface except in summer, when convection clouds are formed.

The time series variability of Earth-like planets is produced by three main factors: the seasonality, by which the energy absorbed (and emitted) changes along the orbit because of the inclination of the rotation axis; the rotation of the planet, as the change in flux is created by the contrast between warm and cold areas of successive planetary views; and the diurnal variability, when the temperature cycle of a particular region produces a change in the emission.

The rotation period of the signal can be retrieved, with a compromise of the length of the time series considered, if cloud lifetimes are longer than the rotation period or if the planet has cloud-convection regions, where clouds are formed constantly. In this case, the regions are characterized for the low brightness temperature from the top of the clouds. The large humidity ratio associated with convection regions is the origin of the periodical signal.

Finally, we have obtain the longitudinal curves of the planets, which allow us to identify warm and cold regions and the influence of the axial tilt (seasons) and eccentricity of the orbit.